



Contents lists available at ScienceDirect

Science Bulletin

journal homepage: www.elsevier.com/locate/scib

Short Communications

How can a youthful mountain survive in a foreland setting? – Constraining the uplift threshold rate by numerical simulation

Haopeng Geng^a, Shun Cai^{a,b}, Honghua Lu^c, Baotian Pan^{a,*}^a Key Laboratory of Western China's Environmental Systems (Ministry of Education), College of Earth and Environmental Sciences, Lanzhou University, Lanzhou 730000, China^b College of Urban and Environmental Sciences, Yancheng Teachers University, Yancheng 224002, China^c Key Laboratory of Geographic Information Science of Ministry of Education, School of Geographic Sciences, East China Normal University, Shanghai 200241, China

ARTICLE INFO

Article history:

Received 20 January 2022

Received in revised form 15 February 2022

Accepted 16 February 2022

Available online xxxxx

© 2022 Science China Press Published by Elsevier B.V. All rights reserved.

Active orogenic belts provide natural laboratories for investigating the mechanisms of tectonic deformation and landscape evolution. Along their foreland basins, the relatively continuous sedimentary archives and varied geomorphic units have documented the history of the tectonic uplift of the adjacent orogenic belts. Geological records (e.g., low-temperature thermochronology and sedimentology) can reveal the history of mountain building on a timescale of tens of millions of years. In contrast, geomorphic evidence generally documents the history of much younger landforms. The northern piedmont of the Chinese Tian Shan is a foreland basin which provides an example of this discrepancy (Fig. 1). In response to the late Cenozoic India-Eurasia collision, the northern piedmont of the Chinese Tian Shan has developed at least three fold-and-thrust belts (Belts I to III, Fig. 1b). Structural Belt II (the Huoerguosi-Manas-Tugulu belt) is one of main active structures controlling the regional topography and tectonic deformation. Previous studies [1–4] have shown that the initiation of the folding of the piedmont anticlines began during the Neogene. In contrast, the available chronologies for the existing, deformed geomorphic surfaces within the anticlines [5,6] imply that the development of the anticlinal topography may have occurred during the Late Pleistocene. This raises the question of why the emergence of the topographic expression of the tectonic deformation lags far behind the initial fold growth in a foreland setting. Addressing this question requires reconstructing the history of surface uplift and the topographic evolution of these piedmont anticlines. Such reconstructions can also help identify the mechanisms controlling the topographic evolution.

Bufe et al. [7] utilized physical experiments to reproduce the growth of an uplifting fold in the southern Chinese Tian Shan foreland. Their results showed that the competition between lateral

channel mobility and the rock uplift rate determines whether the anticlinal topography caused by folding can be preserved. Therefore, the relief creation of anticlines requires an uplift rate that exceeds the rate of lateral erosion. The research of Bufe et al. [7] provides a conceptual model to explain why youthful anticlines emerge among extensive alluvial fan deposits. Previous studies [2,8] have shown that the shortening rates of each anticline in the northern Chinese Tian Shan foreland were less than 1 mm/a on the million-year timescale, but the shortening rates of these structures increased to 1–2 mm/a since the Late Pleistocene. Given the uniform arid environment of the foreland (Fig. S1 online), it is likely that the recent uplift rates could have exceeded the rates of lateral erosion, giving rise to the topographic expression of the piedmont anticlines. The main aim of the present study is to explore the threshold value of the uplift rate in creating the observed topographic relief. However, it is difficult to estimate the uplift rate directly using traditional methods, especially for the rates on a timescale that is not overlapped by the available geochronology. In this study, we use numerical simulation to constrain the uplift history of the studied anticlines. To do this, we first build a landscape evolution model (LEM) to reproduce the topographic evolution of typical areas of the anticlines in Belt II (three target sites are indicated by the white rectangles in Fig. 1b and presented in Fig. S2 online). Then, we constrain the initial uplift time and rate of these youthful mountains based on the similarity principle. Finally, we infer the threshold rate of rock uplift in creating the anticlinal topography across the northern piedmont of the Chinese Tian Shan.

First, we built a two-dimensional LEM with the Landlab platform using the conservation equation (Eq. (1)) to simulate the topographic evolution of the target sites (step1 in Fig. S3 online):

$$\frac{\partial z}{\partial t} = U - (KA^m S^n - c) - D\nabla^2 z, \quad (1)$$

* Corresponding author.

E-mail address: panbt@lzu.edu.cn (B. Pan).<https://doi.org/10.1016/j.scib.2022.03.002>

2095-9273/© 2022 Science China Press Published by Elsevier B.V. All rights reserved.

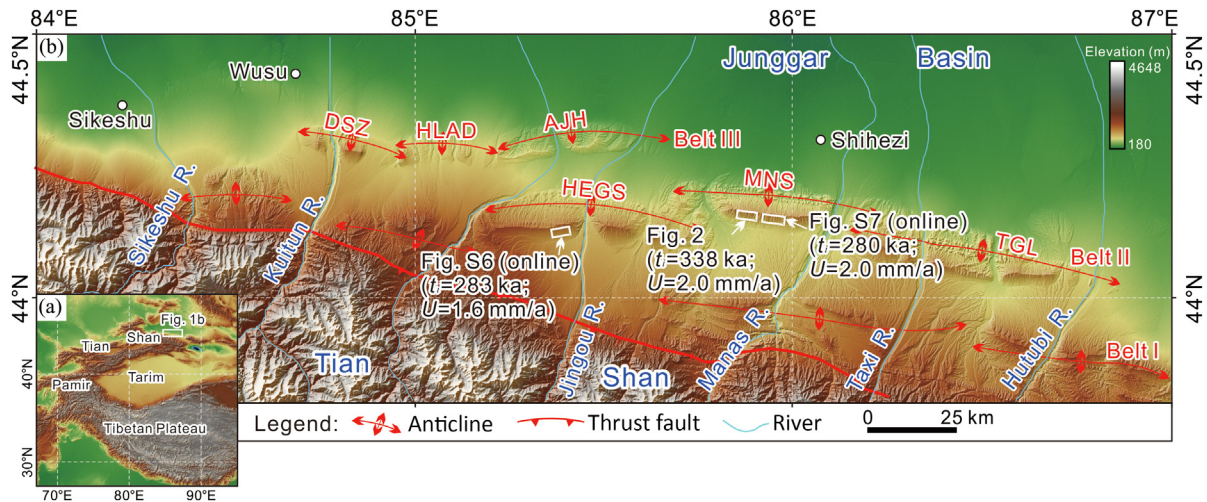


Fig. 1. Map showing the location (a) and topography (b) of the northern piedmont of the Chinese Tian Shan based on a SRTM1-DEM with the resolution of 30 m. The white rectangles in (b) are the three target sites selected for this study (see Fig. S2a–c online). Note that the rock uplift time (t_i) and rate (U) in brackets are results obtained by our simulation approach. DSZ, Dushanzi anticline; HLAD, Halaande anticline; AJH, Anjihai anticline; HEGS, Huoerguosi anticline; MNS, Manas anticline; TGL, Tugulu anticline.

where z is the topographic elevation; t is time; U is the rock uplift rate; K is the dimensional erosion coefficient; m and n are the exponents of the drainage area (A) and the local gradient (S), respectively; and D is the coefficient of diffusion. The term $KA^m S^n$ approximates stream power erosion; c is the erosion threshold and depends on the critical boundary shear stress. We then performed topographic analysis for all the simulated terrains and the realistic terrain (step2 in Fig. S3 online). The main purpose was to compare the similarity and to select a parallel simulated terrain for each realistic terrain. Pan et al. [9] proposed that three topographic variables (local relief, uniform valley spacing, and outlet number) are reliable characteristics for identifying the similarity between simulated and realistic terrains. Local relief (LR) can record the balance between tectonic uplift and erosional processes [10]. Erosion is usually expressed as the competition between advective and diffusive processes; thus, it can be expressed by the uniform valley spacing (UVS) and the outlet number (ON) [11]. Numerical experiments indicate that the model parameters significantly affect the topographic variables of the simulated terrain (Fig. S4 online). The simulation details, including model time (specific time, t_i) and rock uplift rate (U) used in the simulation (step3 in Fig. S3 online) enable us to infer the timing and rate of intense rock uplift for realistic terrain.

Our model takes the precipitation variability into account (Fig. S5 online), which is reasonable in such arid environment. The simulation results show that the timing of intense rock uplift for the Manas anticline was ~ 300 ka, with the uplift rate of ~ 2.0 mm/a (e.g., Fig. 2 for the western part of the southern limb of the Manas anticline). For the Huoerguosi anticline, the timing of intense rock uplift was ~ 280 ka, with the uplift rate of ~ 1.6 mm/a (Fig. S6 online). Our simulation results (Fig. 2 and Figs. S6 and S7 online) are in good agreement with published geological and geomorphic records of the abandonment age of geomorphic surfaces in the northern piedmont of the Chinese Tian Shan [2,5,6] (see details in the Supplementary materials).

Our simulation results suggest that the uplift rate of 1.6 mm/a seems fast enough for the anticlines to survive from sweeping of the antecedent rivers. Given the pre-Late Pleistocene rate of rock uplift of a single anticline of less than 1 mm/a in the northern Chinese Tian Shan foreland, we then infer that the threshold rate of rock uplift could be between 1 and 1.6 mm/a. Under different foreland backgrounds, however, the threshold rate of rock uplift in creating the anticlinal topography may change with varying river discharges and sediment fluxes [7]. The rock uplift threshold rate in creating the topography in a foreland setting can provide a useful reference range for studies of tectonic geomorphology. This

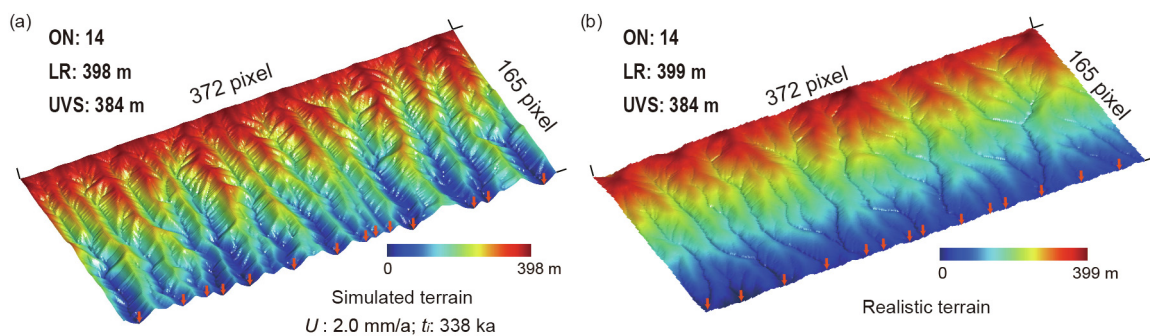


Fig. 2. Topographic characteristics of the simulated and realistic terrains in the western part of the southern limb of the Manas anticline. (a) Simulated terrain for a rock uplift rate of 2.0 mm/a with the model time of 338 ka. (b) Realistic terrain. Relief in the legend is the difference between the elevation of any point in the region and the lowest elevation in the terrain. Pixels are the number of grids with a 12.5 m resolution. UVS is uniform valley spacing; ON is the outlet number; LR is the local relief. The red arrows indicate the outlet locations. The realistic terrain (b) and the simulated terrain (a) have the same ON and UVS, and their LR is very similar. Based on the simulation, the rock uplift rate of ~ 2.0 mm/a was estimated, and the timing of intense rock uplift was constrained to ~ 338 ka.

concept (“uplift threshold”) also has the potential to become an important member of the geomorphic threshold family [12].

The numerical simulation approach used in this work was first applied in the Hexi Corridor, in the northeastern margin of the Tibetan Plateau [9]. The new results presented here further suggest that the approach can reliably reproduce realistic terrain and thereby is able to constrain the uplift history of youthful stage mountains in arid environments. Numerous youthful stage mountains are developed in the foreland basins of active orogenic belts, such as the Himalayan foreland [13] and the foreland of the Zagros Mountains [14]. Therefore, this approach has the potential to be applied in a broader environment (in humid environments in particular) and to become widely-used tool in tectonic geomorphology.

Conflict of interest

The authors declare that they have no conflict of interest.

Acknowledgments

This work was supported by the National Natural Science Foundation of China (41730637, 41971001, and 42071005). We extend our heartfelt thanks to the developers of the Landlab Platform and the module developers of the Earth Surface Processes Modeling Community. We are grateful to Dr. Jan Bloemendal at University of Liverpool for revising the language.

Author contributions

Haopeng Geng and Baotian Pan conceived this study. Haopeng Geng and Shun Cai built the LEM and wrote the original draft. Haopeng Geng and Honghua Lu analyzed the data. All authors contributed to the final manuscript.

Appendix A. Supplementary materials

Supplementary materials to this article can be found online at <https://doi.org/10.1016/j.scib.2022.03.002>.

References

- [1] Charreau J, Chen Y, Gilder S, et al. Neogene uplift of the Tian Shan Mountains observed in the magnetic record of the Jingou River section (Northwest China). *Tectonics* 2009;28:TC2008.
- [2] Deng Q, Feng X, Zhang P, et al. Active tectonics of the Chinese Tianshan Mountains. Beijing: Seismology Press; 2000 (in Chinese).
- [3] Sun J, Zhang Z. Syntectonic growth strata and implications for late Cenozoic tectonic uplift in the northern Tian Shan, China. *Tectonophysics* 2009;463:60–8.
- [4] Hendrix MS, Dumitru TA, Graham SA. Late Oligocene–early Miocene unroofing in the Chinese Tian Shan: an early effect of the India–Asia collision. *Geology* 1994;22:487–90.
- [5] Lu H, Wu D, Zhang H, et al. Spatial patterns of Late Quaternary river incision along the northern Tian Shan foreland. *Geomorphology* 2020;357:107100.
- [6] Yang X, Li A, Hunag W. Uplift differential of active fold zones during the late Quaternary, northern piedmonts of the Tianshan Mountains. *Sci China Earth Sci* 2013;56:794–805.
- [7] Bufe A, Paola C, Burbank DW. Fluvial bevelling of topography controlled by lateral channel mobility and uplift rate. *Nat Geosci* 2016;9:706–10.
- [8] Lu H, Li B, Wu D, et al. Spatiotemporal patterns of the Late Quaternary deformation across the northern Chinese Tian Shan foreland. *Earth Sci Rev* 2019;194:19–37.
- [9] Pan B, Cai S, Geng H. Numerical simulation of landscape evolution and mountain uplift history constrain—A case study from the youthful stage mountains around the central Hexi Corridor, NE Tibetan Plateau. *Sci China Earth Sci* 2021;64:412–24.
- [10] Willett SD, Slingerland R, Hovius N. Uplift, shortening, and steady state topography in active mountain belts. *Am J Sci* 2001;301:455–85.
- [11] Perron JT, Kirchner JW, Dietrich WE. Formation of evenly spaced ridges and valleys. *Nature* 2009;460:502–5.
- [12] Schumm SA. Geomorphic thresholds: the concept and its applications. *Trans Inst Br Geogr* 1979;4:485–515.
- [13] Najman Y, Johnson K, White N, et al. Evolution of the Himalayan foreland basin. *NW India Basin Res* 2004;16:1–24.
- [14] Zebari M, Grützner C, Navabpour P, et al. Relative timing of uplift along the Zagros Mountain Front Flexure (Kurdistan Region of Iraq): constrained by geomorphic indices and landscape evolution modeling. *Solid Earth* 2019;10:663–82.



Haopeng Geng is an associate professor. He works at Key Laboratory of Western China's Environmental Systems (Ministry of Education), College of Earth and Environmental Sciences, Lanzhou University. He received his Ph.D. degree in 2014 from Lanzhou University. His research interest includes surface erosion processes and landscape evolution modeling.



Baotian Pan is a professor. He works at Key Laboratory of Western China's Environmental Systems (Ministry of Education), College of Earth and Environmental Sciences, Lanzhou University. He received his Ph.D. degree in 1991 from Lanzhou University. His research interest includes fluvial processes, landscape evolution, and tectonic geomorphology.